

# Reduction of Cr(VI) to Cr(III) by Wetland Plants: Potential for In Situ Heavy Metal Detoxification

C. MEL LYTLE,<sup>†</sup> FARREL W. LYTLE,<sup>‡</sup>  
NANCY YANG,<sup>§</sup> JIN-HONG QIAN,<sup>†</sup>  
DREW HANSEN,<sup>†</sup> ADEL ZAYED,<sup>†</sup> AND  
NORMAN TERRY\*.<sup>†</sup>

Department of Plant and Microbial Biology,  
111 Koshland Hall, University of California,  
Berkeley, California 94720, The EXAFS Company,  
Pioche, Nevada 89043, and Sandia National Laboratories,  
Division 8714, Livermore, California 94551-0969

Reduction of heavy metals in situ by plants may be a useful detoxification mechanism for phytoremediation. Using X-ray spectroscopy, we show that *Eichhornia crassipes* (water hyacinth), supplied with Cr(VI) in nutrient culture, accumulated nontoxic Cr(III) in root and shoot tissues. The reduction of Cr(VI) to Cr(III) appeared to occur in the fine lateral roots. The Cr(III) was subsequently translocated to leaf tissues. Extended X-ray absorption fine structure of Cr in leaf and petiole differed when compared to Cr in roots. In roots, Cr(III) was hydrated by water, but in petiole and more so in leaf, a portion of the Cr(III) may be bound to oxalate ligands. This suggests that *E. crassipes* detoxified Cr(VI) upon root uptake and transported a portion of the detoxified Cr to leaf tissues. Cr-rich crystalline structures were observed on the leaf surface. The chemical species of Cr in other plants, collected from wetlands that contained Cr(VI)-contaminated wastewater, was also found to be Cr(III). We propose that this plant-based reduction of Cr(VI) by *E. crassipes* has the potential to be used for the in situ detoxification of Cr(VI)-contaminated wastestreams.

## Introduction

The novel technology of phytoremediation embraces plant accumulation processes for the cleanup of toxic heavy metals and organic chemicals (1, 2). Several plant species have been identified that are excellent hyperaccumulators of a number of heavy metals, e.g., *Brassica juncea* (Indian mustard) (3, 4) and *Thlaspi caerulescens* (Alpine pennycress) (5). Other species including *Myriophyllum brasiliense* (Parrot's feather) (6), *Salix* sp. (willow), and *Populus* sp. (poplar) have also demonstrated phytoremediating abilities (7).

A potentially significant approach to heavy metal remediation is the use of plants that detoxify metals in situ through plant-based chelation, reduction, and/or oxidation mechanisms. For example, *Potamogeton pectinatus* (Sago pondweed) detoxified high concentrations of accumulated manganese when aqueous Mn(II) absorbed by the roots was oxidized to a nontoxic manganese(III) oxide in leaf tissues

over the growing season (8, 9). It was also demonstrated that cadmium in the xylem sap of *B. juncea* was chelated by oxygen (organic acids) and sulfur ligands (phytochelatin) in the transport, accumulation, and detoxification of Cd (4). Recent studies have found that selenium detoxification in a constructed wetland receiving selenite-contaminated refinery wastewater may be due in part to wetland plant-based reduction of toxic selenite to nontoxic dimethylselenide gas (10).

Chromium has many industrial uses, and its unregulated application has led to the contamination of soil, sediment, surface waters, and groundwaters (11). Hexavalent chromium was classified as a primary contaminant because of its mobility in soil and groundwater and its reported harmful effects on organisms including humans (12). Within living cells, Cr(VI) induces cancer and mutation by damaging DNA—protein cross-links and by causing single-strand breaks (13). Cr(III), on the other hand, is stable, nontoxic, and listed as an essential element for the good health and nutrition of many organisms (14).

Because the reduction of toxic Cr(VI) leads to the formation of stable, nontoxic Cr(III), it is important to study how this reduction may be implemented so as to achieve detoxification and therefore environmental cleanup in situ. Reduction of Cr(VI) can be accomplished abiotically by reactions with aqueous ions, by electron transfer at mineral surfaces, by reduction with humic substances and other organic molecules, and by lyophilized plant tissue (15, 16). More importantly, from the point of view of environmental cleanup, the reduction of Cr(VI) can be mediated biologically by various enzymes and nonenzymatic agents (17, 25); enzymes include cytochrome P-450 reductase, NAD(P)H quinone reductase, glutathione reductase, and aldehyde oxidase (17–21).

Microbial reduction of Cr(VI) to Cr(III) has been demonstrated (26–28). A NADPH-dependent Cr reductase capable of Cr(VI) detoxification was purified from the bacterium *Pseudomonas ambigua* G-1 (29). Several studies indicate that plants have the ability to reduce Cr(VI) (30–34). Some of these studies were conducted using speciation techniques that required chemical extraction of plant materials before determination of the Cr species in the plant tissue; however, such sample preparation procedures may alter the speciation resulting in artifacts. To eliminate sample preparation artifacts, we used a synchrotron-based X-ray absorption spectroscopy technique to speciate Cr in untreated live plant tissues of *Eichhornia crassipes* (water hyacinth), a wetland plant that is frequently planted into constructed wetland treatment systems containing heavy metal-contaminated wastewater. Our objective was to determine whether *E. crassipes* and other wetland plant species can reduce toxic Cr(VI) to nontoxic Cr(III) and subsequently accumulate detoxified Cr into leaf and root tissues.

## Materials and Methods

**Plant Collection, Growth Conditions, and Cr(VI) Treatments.** *E. crassipes* was collected in September 1995 from the lower San Joaquin River, San Joaquin County, CA. From this parent population, replicate daughter plants were grown under greenhouse conditions in quarter-strength Hoagland nutrient solution. The nutrient solutions were supplied with 10  $\mu\text{g mL}^{-1}$  Cr(VI) as potassium dichromate ( $\text{K}_2\text{Cr}_2\text{O}_7$ ) and buffered to pH  $7.3 \pm 0.2$ . In basic solution (pH > 6), the tetrahedral chromate ion,  $(\text{CrO}_4)^{2-}$  is formed; between pH 2 and pH 6,  $(\text{HCrO}_4)^-$  and the dichromate ion  $(\text{Cr}_2\text{O}_7)^{2-}$  are in

\* Corresponding author phone: (510)642-3510; fax: (510)642-4995; e-mail: nterry@nature.berkeley.edu.

<sup>†</sup> University of California, Berkeley.

<sup>‡</sup> The EXAFS Company.

<sup>§</sup> Sandia National Laboratory.

equilibrium, and under more acidic conditions ( $\text{pH} < 1$ ), the main Cr species in solution is  $\text{H}_2\text{CrO}_4$  (35). Given the Cr solution equilibria, the Cr species in the Cr(VI)-treated nutrient solutions in our experiments was the  $\text{Cr(VI)O}_4^{2-}$  ion. The Cr(VI) treatments ranged from 4 h to 14 days in separate experiments over 9 months. In all experiments, *E. crassipes* leaves were never in contact with the nutrient culture solutions to avoid precipitation of Cr on leaf surfaces.

Antimicrobial agents, rifampicin ( $20 \mu\text{g mL}^{-1}$ ) and amphotericin B ( $5 \mu\text{g mL}^{-1}$ ) (Sigma Chemical Company), were added to experiment nutrient solutions as a pretreatment for 1 week prior to each Cr(VI) treatment and during the experiments separately and in combination to determine if a possible plant/microbe association was responsible for Cr(VI) reduction. Rifampicin was selected as a treatment antibiotic because it was found to be highly effective in controlling Cr(VI)-tolerant bacteria that were isolated from metal-processing waste evaporation ponds (36). Amphotericin B is a broad-range antimycotic and was used to control possible yeast and mold populations in nutrient culture solutions. The antibiotic treatments would inhibit possible interference caused by the microbial reduction of Cr(VI) in the nutrient solution or on root surfaces. The control of microbial populations during the Cr(VI) treatment experiments would lead to the characterization of a plant-based Cr(VI) reduction capability.

To determine the possible location of Cr(VI) reduction, living intact *E. crassipes* plants were supplied with  $100 \mu\text{g mL}^{-1}$  Cr(VI) with antibiotic additions and remained in nutrient culture up to 72 h for in situ X-ray spectroscopy analyses. X-ray spectra for living plants were collected at intervals of 4, 24, and 72 h. The beam size used to measure XAS on living plants had an approximately 1 mm vertical and 20 mm horizontal size.

To gain insight into the possible reduction of Cr(VI) by plants other than *E. crassipes* and to evaluate the potential field application of this plant-based reduction process, we collected plant tissues from other wetland plant species: *Typha latifolia* (cattail), *Scirpus maritimus* (saltmarsh bulrush), and *Polypogon monspeliensis* (rabbitfoot grass). Shoots and roots were collected for analysis with X-ray spectroscopy in October 1995 from a constructed wetland that treated refinery wastewater contaminated with Cr(VI) (10).

**Analysis of Cr in *E. crassipes* Tissues.** Plant tissues were analyzed for Cr to detect differences in accumulated Cr content between leaf and root tissues. Plant samples were rinsed in deionized water, dried at  $70^\circ\text{C}$ , weighed, and ground in a Wiley Mill to pass a 40-mesh screen; 100 mg samples were digested with  $\text{HNO}_3/\text{HCl}$ . Chromium concentrations were measured with ICP-AES according to EPA Method 6010 (37).

**X-ray Absorption Spectroscopy Analysis and Data Collection.** We used X-ray absorption spectroscopy (XAS) to detect the chemical speciation of Cr in plant tissues supplied with Cr(VI). To prepare samples for XAS analysis, leaf and root tissues of *E. crassipes*, *T. latifolia*, *S. maritimus*, and *P. monspeliensis* were triple-rinsed in deionized water, frozen in liquid nitrogen, ground to a fine texture, and stored at  $-80^\circ\text{C}$ . XAS analyses of frozen and living plant tissues were completed at the Stanford Synchrotron Radiation Laboratory (SSRL) on Beam Line 4-1. The electron energy was 3.0 GeV with a current of  $\approx 50$ – $100$  mA. Monochromatic X-rays from a Si(111) double-crystal spectrometer were detuned 50% for harmonic rejection and positioned with a 1-mm entrance slit that produced a beam of  $\approx 1$  eV bandwidth at the Cr K-edge. Frozen leaf, petiole and root tissues, and intact living plants were placed in a sample chamber at a  $45^\circ$  angle to the X-ray beam. Fluorescent X-ray spectra of Cr in plant tissues were obtained by a series of replicate scans (3–20) dependent on Cr concentration. Plant tissue Cr concentrations ranged

TABLE 1. Chromium Content in *E. crassipes* Leaf and Root Tissues Supplied with  $10 \mu\text{g mL}^{-1}$  Cr(VI) (–ABF), +Antibacterial (+AB), +Antifungal (+AF), and in Combination (+ABF) over 14 Days<sup>a</sup>

treatment	leaf ( $\text{mg kg}^{-1}$ dry wt)	root ( $\text{mg kg}^{-1}$ dry wt)
–ABF	$89 \pm 27\text{a}^b$	$5265 \pm 610\text{a}$
+AB	$96 \pm 28\text{a}$	$5970 \pm 410\text{a}$
+AF	$55 \pm 5\text{a}$	$4890 \pm 740\text{a}$
+ABF	$72 \pm 18\text{a}$	$5360 \pm 440\text{a}$

<sup>a</sup> Element concentration expressed as mean  $\pm$  standard error of mean,  $n = 4$ . <sup>b</sup> Means followed by the same letter are not significantly different ( $P \leq 0.05$ ).

well within the resolution range of the XAS technique, and the data were of excellent quality. Spectra were also collected for Cr(VI), Cr(V), and Cr(III) reference compounds and solutions. The energy positions of all spectra were calibrated against a Cr reference foil.

**Scanning Electron Microscopy of *E. crassipes* Leaf Surfaces.** Scanning electron microscopy with energy-dispersive X-ray (SEM/EDX) was used to detect the location of accumulated Cr(III) in *E. crassipes* leaf and root tissues. To prepare tissues for SEM/EDX, leaves and roots were harvested, triple-rinsed in deionized water, and dried at  $35^\circ\text{C}$  for 1 week. Air-dry tissues were prepared metallographically when mounted in cold epoxy, cross-sectioned, and polished. Mounted samples were carbon-coated and analyzed with a JEOL 840 scanning electron microscope with energy dispersive system at Sandia National Laboratory, Livermore, CA.

## Results and Discussion

**Cr Accumulation in the Presence of Antibiotics.** Most of the Cr taken up by *E. crassipes* supplied with Cr(VI) at  $10 \text{ mg L}^{-1}$  was accumulated in plant roots; much less was accumulated in shoots (Table 1). The presence or absence of antibiotics in the culture solution did not affect the concentration of Cr in plant tissues ( $P \leq 0.05$ ) (Table 1). It would appear therefore that *E. crassipes* could take up and translocate Cr regardless of whether microbes were present or not.

**Reduction of Cr(VI) by *E. crassipes*.** The comparison of the X-ray absorption near-edge structure (XANES), i.e., valence and local coordination symmetry (38, 39) of Cr in *E. crassipes* with 0.1 M  $[\text{Cr(III)} \cdot (\text{H}_2\text{O})_6]$  and 0.1 M  $[\text{Cr(VI)O}_4]^{2-}$  reference solutions, showed that the valence of Cr in leaf, petiole, and root tissues was like the Cr(III) reference solution (Figure 1A). This was illustrated by the lack of a prepeak and positive shift along the energy axis of the *E. crassipes* tissues when compared to the Cr(VI) reference. These data provide clear evidence that Cr(VI) is reduced to Cr(III) in *E. crassipes* tissues. Since the Cr(VI) reduction occurred in the presence of antibiotics, these results show that *E. crassipes* was able to reduce Cr(VI) to Cr(III) without the assistance of Cr-reducing microbes in the nutrient solution or rhizosphere (Figure 1B). That no microbial reduction of Cr(VI) to Cr(III) took place in the nutrient culture during the course of the experiment was further demonstrated by the fact that XAS speciation of Cr in nutrient culture solutions before and after plant addition to the antibiotic-amended solutions revealed the presence of Cr(VI) species only (data not shown). Furthermore, there was no evidence of microbial colonization [after Cr(VI) and antibiotic treatments] as shown by SEM of *E. crassipes* root surfaces.

To locate the site of Cr(VI) reduction and to determine the valence of translocated Cr, living intact *E. crassipes* plants were supplied with Cr(VI) and placed directly into the X-ray

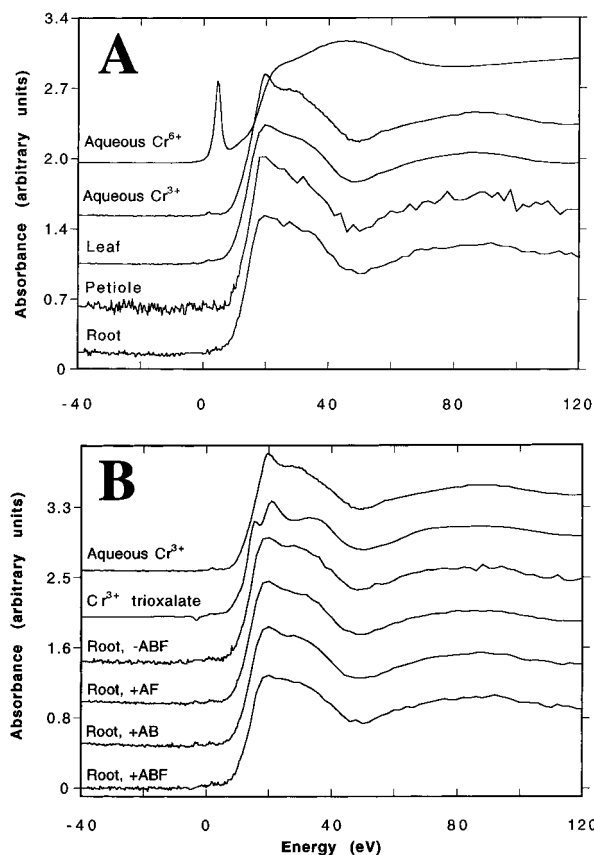


FIGURE 1. (A) Comparison of the Cr K-edge XANES of *E. crassipes* tissues with 0.1 M  $[\text{Cr}(\text{III})\cdot(\text{H}_2\text{O})_6]$  and  $[\text{Cr}(\text{VI})\text{O}_4]^{2-}$  reference solutions. The differences in the noise level of the data of *E. crassipes* tissues was a function of Cr concentration. (B) Cr K-edge XANES for *E. crassipes* root tissues supplied with Cr(VI) showing the effects of antibiotic treatments: no antibiotics (-ABF), +20  $\mu\text{g mL}^{-1}$  rifampicin (+AB), +5  $\mu\text{g mL}^{-1}$  amphotericin B (+AF), and in combination (+ABF) on the speciation of accumulated Cr as compared to 0.1 M  $[\text{Cr}(\text{III})\cdot(\text{H}_2\text{O})_6]$  and  $[\text{K}_3\text{Cr}(\text{C}_2\text{O}_4)_3\cdot 3\text{H}_2\text{O}]$  (chromium(III) trioxalate) references. The spectra have been offset vertically for clarity.

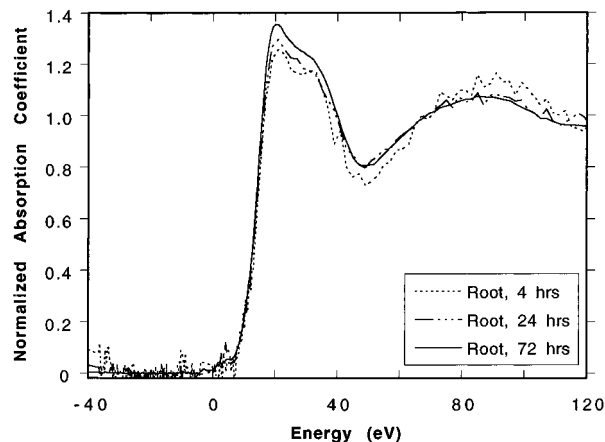


FIGURE 2. Cr K-edge XANES of living intact *E. crassipes* roots after 4, 24, and 72 h exposure to 100  $\mu\text{g mL}^{-1}$  Cr(VI). Note the absence of a pre-peak or shift to more positive energy that would be characteristic of Cr(VI) XANES.

beam while on-line at SSRL. Within 4 h, we detected measurable Cr(III) in the fine lateral roots but not in the main root system. The K-edge XANES of Cr in this root tissue showed that the Cr(VI) supplied in the nutrient solution had been reduced to Cr(III) during root uptake (Figure 2). After 24 h, Cr was present as Cr(III) in all roots; within this period,

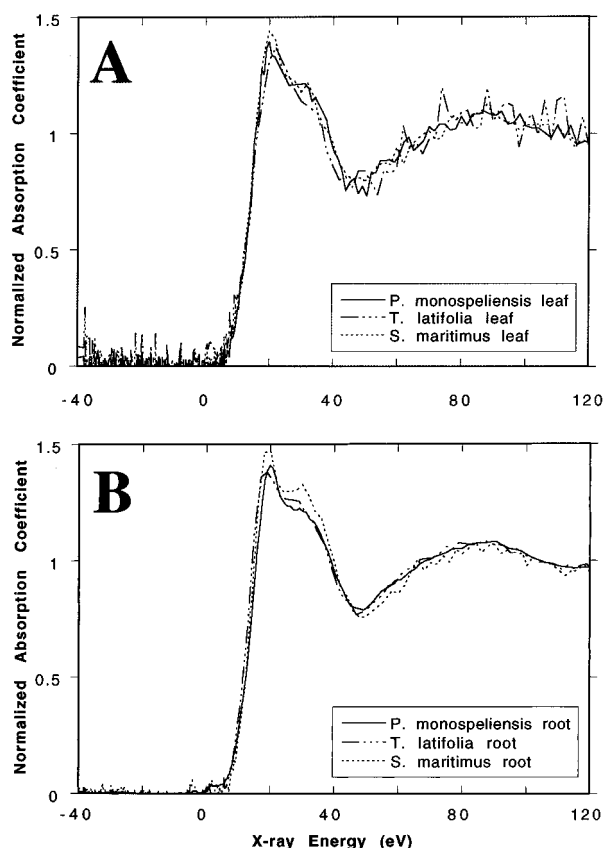


FIGURE 3. (A) Cr K-edge XANES of *T. latifolia*, *S. maritimus*, and *P. monspeliensis* leaf tissues from a constructed wetland that received Cr(VI)-contaminated wastewater. (B) Cr K-edge XANES of *T. latifolia*, *S. maritimus*, and *P. monspeliensis* root tissues. Note the absence of a pre-peak or shift to more positive energy that would be characteristic of Cr(VI) XANES.

some Cr(III) was translocated to the petiole. By 72 h, Cr(III) was present in all plant tissues although at varying concentrations. These results show that Cr(VI) was rapidly reduced during uptake by the fine lateral roots and then translocated at a slower rate as Cr(III) through the main roots to the leaves.

It is not clear how plants take up and reduce Cr(VI) into Cr(III) in the fine roots. Plants have been shown to reduce iron from Fe(III) to Fe(II) by a membrane-bound iron(III) reductase, prior to uptake (30, 40). A similar mechanism may exist for Cr; a membrane-bound chromium reductase has been found in bacteria (29) but not, as yet, in plants. There is evidence of Cr(VI) to Cr(III) reduction in plant tissues. Lyon et al. (31) found that *Leptospermum scoparium* (New Zealand tea tree) cultured in solutions with  $\text{Na}_2^{51}\text{CrO}_4$  accumulated most of the absorbed radioactivity in the roots; about 30% of the radioactivity was soluble in 80% ethanol in the form of three  $^{51}\text{Cr}$  complexes with the majority being identified as a trioxalatochromate [Cr(III)] ion. These complexes were also found in stem and leaf tissues.

Plant uptake of Cr(VI) has also been investigated using ESR spectroscopy. One study showed that, after the absorption of Cr(VI) by *Allium sativum* (garlic), the first Cr species produced was mobile Cr(V), where the metal ion was bound to low-molecular weight ligands; this was followed by the formation of Cr(III) species (32). Other studies with ESR spectroscopy showed that when green algae (*Spirogyra* and *Mougeotia*) and two crop species were incubated with Cr(VI), it generated both Cr(V) and Cr(III) species (33). Because of its high toxicity, the generation of Cr(V) by plant reduction of Cr(VI) would have serious consequences for various ecological cycles. However, in our research we did

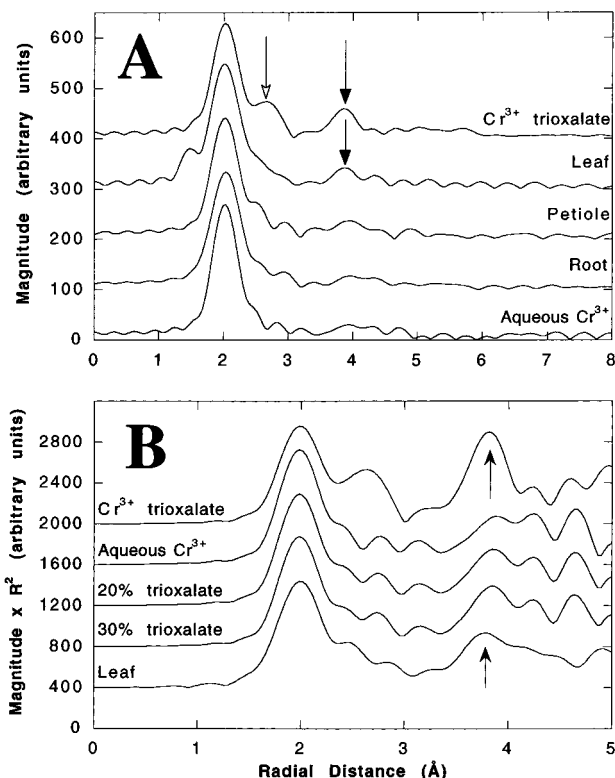


FIGURE 4. (A) Comparison of the Fourier transforms of the Cr–O phase-shifted and  $K^2$ -weighted EXAFS of *E. crassipes* tissues with that of the 0.1 M Cr(III) solution and the chromium(III) trioxalate compound. Note that the abscissa is a radial distance scale with the Cr atom that absorbed the X-ray at the origin. The 2nd (open arrow) and 3rd (closed arrow) peaks at  $\approx 2.7$  and  $\approx 3.8$  Å in the oxalate transform are characteristic of Cr(III) bonding to the oxalate ligand. The petiole and leaf tissues were quite similar to each other and slightly different from the root tissue. (B) Phase-corrected Fourier transforms of Cr K-edge EXAFS of chromium(III) trioxalate and 0.1 M Cr(III) blended in proportions indicated. The magnitude of the transform has also been multiplied by  $R^2$  in order to amplify the more distant bonds. There was a match with the *E. crassipes* leaf tissue at  $\approx 20$ – $30\%$  oxalate (closed arrow).

not detect the presence of a Cr(V) intermediate in any plant tissues; comparison of the XANES of Cr in leaf, petiole, and root tissues with Cr(VI), Cr(V), and Cr(III) references yielded no indication that the intermediate valence form Cr(V) accumulated in *E. crassipes* during any of the experiments to a XAS detection limit of  $\approx 1.0 \mu\text{g g}^{-1}$ . Our research differed significantly from those studies that revealed the presence of a Cr(V) intermediate (32, 33). In both of these studies, the investigators used 4–5-day-old seedlings supplied with Cr(VI) concentrations ranging from 250 down to  $8 \text{ mg L}^{-1}$  [at  $8 \text{ mg L}^{-1}$ , the Cr(V) signal had almost disappeared; 32] and  $208 \text{ mg L}^{-1}$  (33); furthermore, there was no attempt to control microbial reduction. In our study, we used fully developed mature plants provided with antibiotics to control microbial reduction and supplied with lower Cr(VI) concentrations of 10 and  $100 \text{ mg L}^{-1}$ . In fact, when XAS was used for speciation of Cr in *B. juncea* plants supplied with a solution of Cr(VI), the roots were found to contain Cr(III), although no data were shown (D. Salt, unpublished, cited in ref 34).

**Reduction of Cr(VI) to Cr(III) by Other Wetland Plant Species.** The K-edge XANES of Cr in both shoot and root tissues of the wetland species (*T. latifolia*, *S. maritimus*, and *P. monspeliensis*), which were collected from a constructed wetland that received Cr(VI)-contaminated wastewater, were very similar to Cr(III) in *E. crassipes* and the Cr(III) reference solution (Figure 3A,B). In these species, there was no

TABLE 2. List of Fourier Transform Structural Parameters and Least-Squares Fits to EXAFS Data for Cr References and Accumulated Cr in *E. crassipes* Tissues<sup>a</sup>

sample	$N \pm 1$	$R \pm 0.02 \text{ \AA}$	$\sigma^2 (\text{\AA}^2)$
Reference Compounds			
$\text{Cr}_2\text{O}_3$ ( $R = 2.012$ ) <sup>b</sup>	5.9	2.015	0.0041
$\text{Cr}_2\text{FeO}_4$ ( $R = 2.053$ ) <sup>b</sup>	5.2	2.020	0.0014
$\text{CrVO}_4$ ( $R = 2.004$ ) <sup>b</sup>	6.8	1.996	0.0072
$\text{Cr}(\text{NO}_3)_3 \cdot \text{H}_2\text{O}$ <sup>c</sup>	5.1	1.99	0.0030
$\text{K}_3\text{Cr}(\text{C}_2\text{O}_4)_3 \cdot 3\text{H}_2\text{O}$ <sup>c</sup>	6.0	2.00	0.0039
Reference Solutions <sup>d</sup>			
0.1 M Cr(III)	6.3	2.00	0.0028
0.01 M Cr(III)	7.9	2.00	0.0078
<i>E. crassipes</i> Tissues			
root	6.6	2.00	0.0052
petiole	5.9	2.00	0.0030
leaf	7.0	2.00	0.0054

<sup>a</sup> The coordination number ( $N$ ), bond length ( $R$ ), and mean-squared relative displacement ( $\sigma^2$ ) are from least-squares fit. <sup>b</sup> Known distance from X-ray diffraction. <sup>c</sup> Complete crystal structures are unknown. <sup>d</sup> Cr(III) aqueous solutions prepared from  $[\text{Cr}(\text{NO}_3)_3 \cdot 9\text{H}_2\text{O}]$ .

evidence that Cr(VI) had accumulated in shoot or root tissues over the growing season (Figure 3A,B). This suggests that other wetland species were able to reduce Cr(VI) to Cr(III) under constructed wetland conditions. Furthermore, it was found using XAS that a number of vegetable crop species treated with Cr(VI) were able to reduce Cr(VI) to Cr(III) in root tissues (41).

**Characterization of Reduced Cr in *E. crassipes*.** We characterized the reduced Cr in *E. crassipes* by analyzing the extended X-ray absorption fine structure (EXAFS). From this technique, we were able to develop structural information of Cr in plant tissues, i.e., local bond distances ( $R$ ), coordination number ( $N$ ), the chemical identity of coordinating atoms, and a measure of total disorder ( $\sigma^2$ ) (39, 42). This analysis proceeded by first calculating Cr–O backscattering and phase shift parameters with FEFF (43). Calculation of the  $K^2$ -weighted Fourier transforms using the Cr–O phase shift produced the radial structure functions shown for plant tissues and reference compounds (Figure 4). In Figure 4A, the first coordination shell at 2 Å was essentially identical for leaf, petiole, root, and the Cr references (Figure 4A); this would indicate that Cr(III) was bound to oxygen in all tissues.

With respect to the second and third peaks at 2.7 (Figure 4A, open arrow) and 3.8 Å (closed arrow), there were differences among the plant tissues. The second and third peaks did not appear in the root but did appear in the petiole and more so in the leaf tissues (Figure 4A). These data suggest the following. Cr(III) in roots was surrounded by water molecules (similar to the Cr(III) reference solution); however, the speciation of Cr appeared to change after translocation to the leaf. Within the leaf, Cr(III) EXAFS were more similar to the chromium(III) trioxalate reference [i.e.,  $\text{K}_3\text{Cr}(\text{C}_2\text{O}_4)_3 \cdot 3\text{H}_2\text{O}$ ] than other Cr references. This suggests that Cr(III) may be bound by oxalate ligands as was found with *L. scoparium* (31).

We obtained an estimate of the amount of Cr(III) bound to oxalate in the leaf by adding together the transforms of the chromium(III) trioxalate reference and the 0.1 M Cr(III) reference solution in varying proportions to simulate the transform observed for leaf tissue (Figure 4B). The blended transforms suggest that about 20–30% of the Cr in the leaf may be bound to oxalate (Figure 4B; closed arrow).

To quantify the structural information obtained from the EXAFS, we selected the area of the first coordination sphere ( $\approx 1.3$ – $2.4$  Å) and back-transformed the function to get the EXAFS for the first coordination sphere only. This function was fitted by a least-squares algorithm (44). To determine

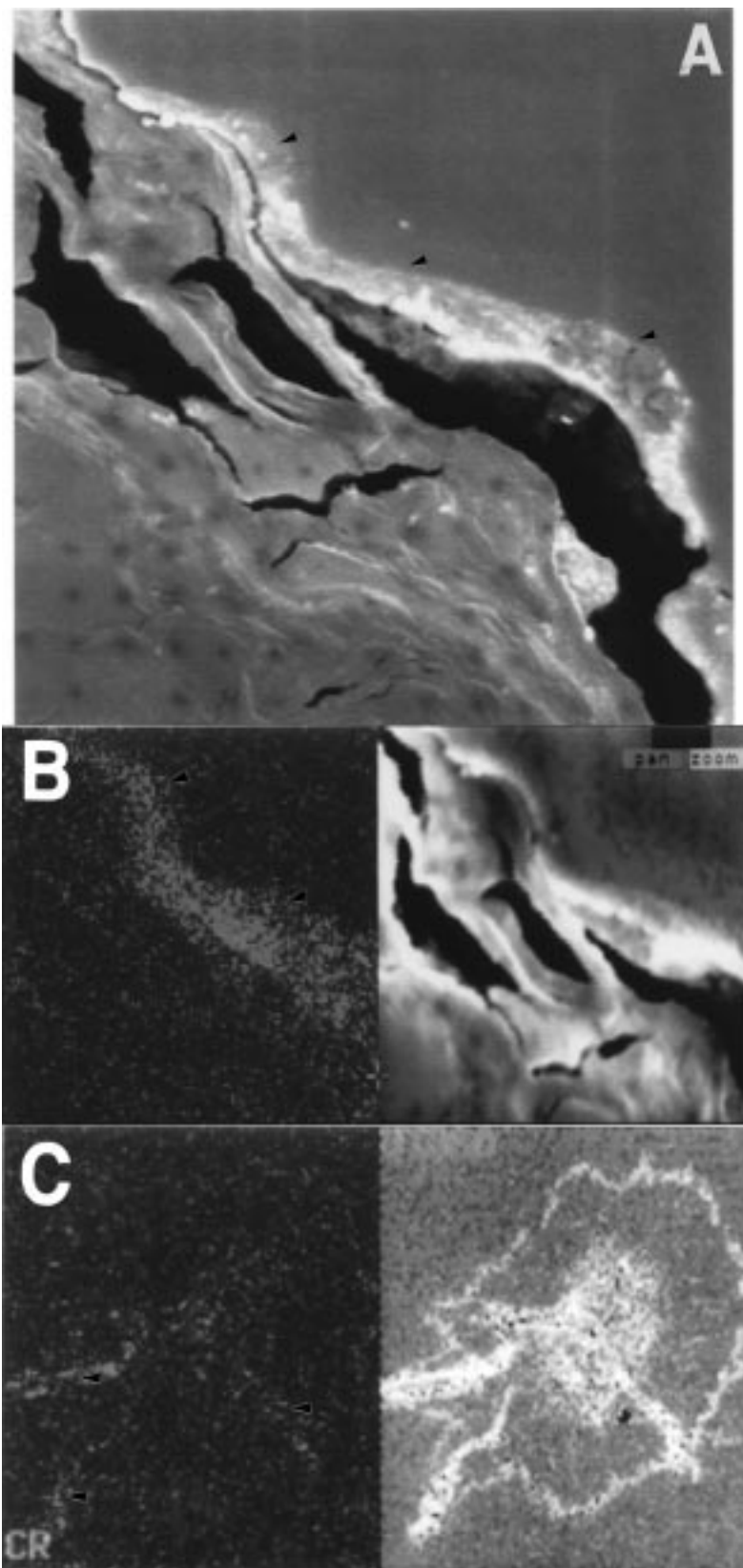


FIGURE 5. (A) SEM micrograph of cross-sectioned *E. crassipes* leaf supplied with Cr(VI) over 14 days. Note the presence of small crystalline structures along the under-leaf surface (closed arrows). (B) SEM/EDX color map of cross-sectioned *E. crassipes* leaf tissue showing the association of Cr (red color) with the crystal structures on the leaf surface (closed arrows; scale bar, 8  $\mu\text{m}$ ). (C) SEM/EDX color map of cross-sectioned *E. crassipes* root tissue showing Cr (red color) associated with the fine-lateral root tissues.

$N$ ,  $R$ , and  $s^2$ , input into the algorithm along with the data were the FEFF Cr–O backscattering and phase shift parameters that contained two unknown factors,  $E_0$  and  $S_0^2$  that

must be calibrated by fitting to EXAFS from standard compounds.  $E_0$  aligns the muffin tin zero of energy with that of the experiment and has an effect on the value of  $R$ .

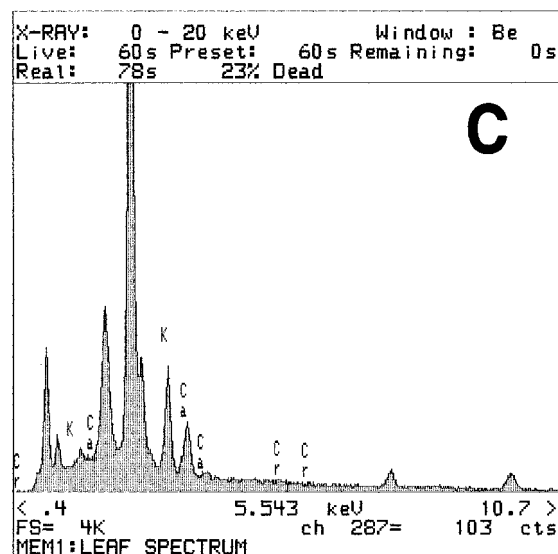
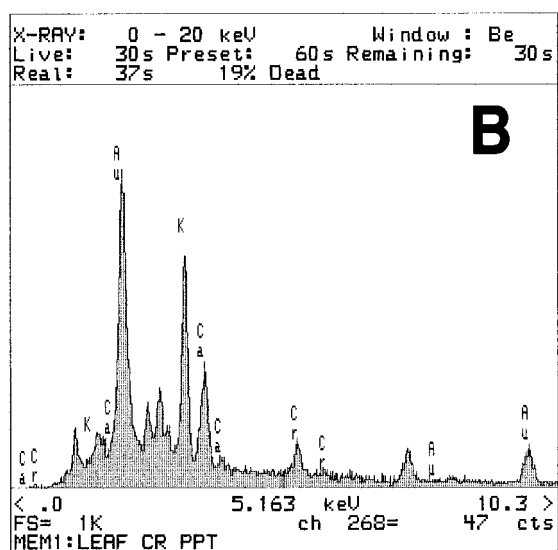
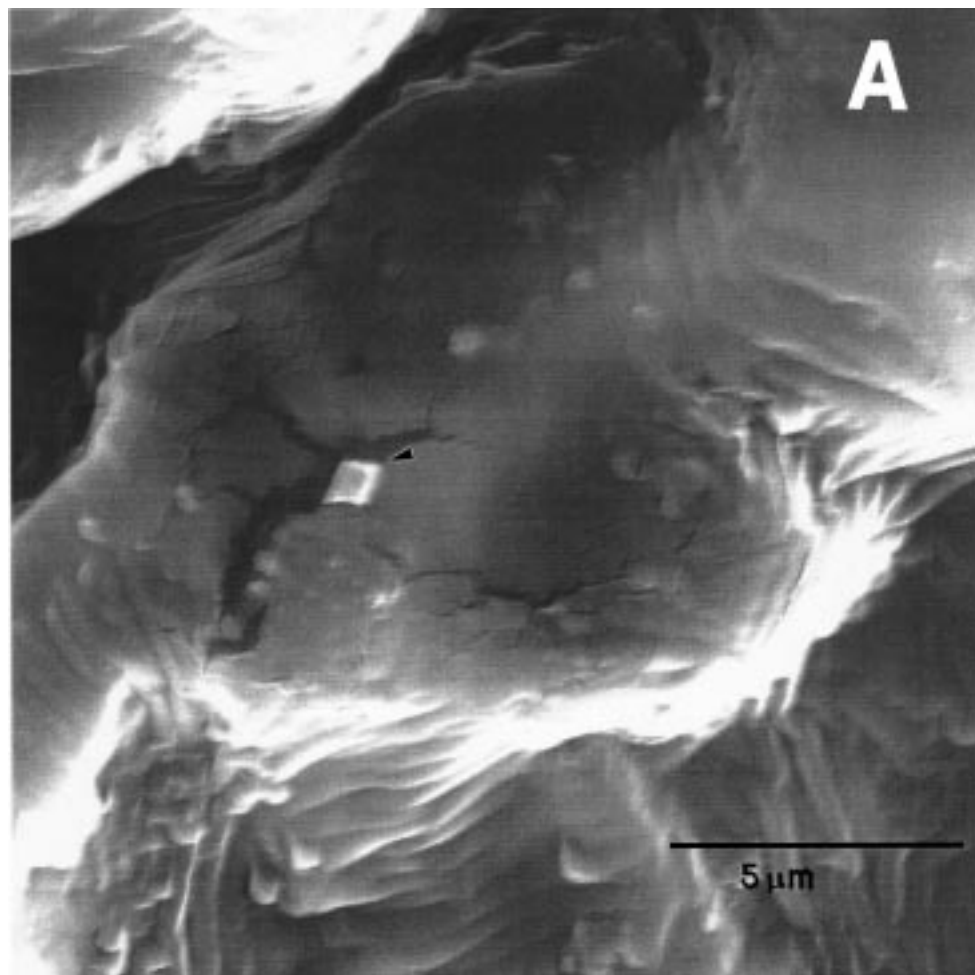


FIGURE 6. SEM micrograph of *E. crassipes* leaf tissue showing close-up of small crystalline structures along the leaf surface (closed arrow; scale bar, 5  $\mu$ m). (B) SEM/EDX spectra of a crystalline structure on *E. crassipes* leaf surface after Cr(VI) treatment (note the presence of Cr peaks in the spectra). (C) SEM/EDX spectra of *E. crassipes* leaf tissue without Cr(VI) treatment.

$S_0^2$  is a multiple electron term that scales the coordination number. We used electron yield data from powder preparations of  $\text{Cr}_2\text{O}_3$ ,  $\text{Cr}_2\text{FeO}_4$ , and  $\text{CrVO}_4$  to determine that  $E_0 = 12.2$  eV and  $S_0^2 = 0.95$ . Values of  $\sigma^2$  were characteristic of each material. From this calibration, we estimated error values for *E. crassipes* tissues (Table 2). Complete crystal

structure parameters were not known for  $[\text{Cr}(\text{NO}_3)_3 \cdot 9\text{H}_2\text{O}]$  and  $[\text{K}_3\text{Cr}(\text{C}_2\text{O}_4)_3 \cdot 3\text{H}_2\text{O}]$  except that Cr was in octahedral coordination by oxygen (45, 46). The results of the fitting of the first coordination sphere of the reference compounds, Cr(III) solutions, and plant tissues clearly show that, in root, petiole, and leaf, Cr is bound in octahedral oxygen coordina-

tion and that the bond distances are identical to those of the 0.1 M Cr(III) reference solution (Table 2). This again indicates that Cr(VI) supplied to *E. crassipes* roots was reduced to Cr(III) and that Cr(III) was translocated to petiole and leaf tissues.

A portion of the accumulated Cr appears to be bound to oxalate in the leaves, and some of it may eventually be secreted as crystalline structures in and on leaf surfaces. SEM micrographs of *E. crassipes* leaf surfaces detected crystalline structures (Figure 5A–C) along the underside of the leaf surface. When SEM/EDX spectra of these structures were collected, they were found to contain a high Cr concentration (Figure 6A–C). This suggests that chromium oxalate crystals may have formed on the leaf surface of *E. crassipes* as Cr accumulated in leaf tissues. Oxalate is a common ligand in many plants, and in particular, calcium oxalates in leaves can form extensive crystal bundles. It has been suggested that metal-rich crystalline structures in the vacuoles of *Larrea tridentata* (Creosote bush), grown near a smelting site, may be responsible for the immobilization of copper in leaf tissues (47).

**Phytoremediation of Cr by *E. crassipes*.** *E. crassipes* accumulated substantial amounts of Cr, especially in roots (about 5000–6000 mg kg<sup>-1</sup> after supplying 10 mg L<sup>-1</sup> for a period of 14 days) (Table 1). *E. crassipes* is a floating aquatic plant that can easily be harvested from a treatment lagoon or constructed wetland (48, 49). We conclude that water hyacinth has an excellent potential for the phytoremediation of Cr in wastewater because (i) it has the ability to absorb and remove toxic Cr(VI) and then reduce it to nontoxic Cr(III); (ii) it can accumulate Cr in high concentrations in its tissues, especially roots; (iii) it produces very large amounts of biomass (106–165 t ha<sup>-1</sup> yr<sup>-1</sup>; 50); and (iv) it may be easily harvested in the whole plant form thereby including the substantial amount of Cr in the roots. Thus, the Cr(VI) reduction/detoxification process of *E. crassipes* and other wetland plants has the potential to be utilized for the in situ remediation of Cr(VI)-contaminated groundwater, sediments, and industrial wastestreams.

## Acknowledgments

This study was supported by the Electric Power Research Institute and Pacific Gas and Electric Company. We thank the U.S. Department of Energy and SSRL for granted beam time (Proposal 2413Mp) and on-line technical support as well as the Sandia National Laboratory, which provided facilities for the electron microscopy.

## Literature Cited

- Cunningham, S. D.; Berti W. R.; Huang, J. W. *Trends Biotechnol.* **1995**, *13*, 393.
- Cunningham, S. D.; Ow, D. W. *Plant Physiol.* **1996**, *110*, 715.
- Salt, D. E.; Blaylock, M.; Kumar, N.; Dushenkov, V.; Ensley, B.; Chet, I.; Raskin, I. *Bio/Technology* **1995**, *13*, 468.
- Salt, D. E.; Pickering, I. J.; Prince, R. C.; Gleba, D.; Dushenkov, S.; Smith, R. D.; Raskin, I. *Environ. Sci. Technol.* **1997**, *31*, 1636.
- Brown, S. L.; Chaney, R. L.; Angle, J. S.; Baker, A. J. M. *J. Environ. Qual.* **1994**, *23*, 1151.
- Brown, K. S. *BioScience* **1995**, *45*, 579.
- Black, H. *Environ. Health Perspect.* **1995**, *103*, 1106.
- Lytle, C. M.; Smith, B. N. *Great Basin Nature* **1995**, *55*, 164.
- Lytle, C. M.; Lytle, F. W.; Smith, B. N. *J. Environ. Qual.* **1996**, *25*, 311.
- Hansen, D.; Duda, P. J.; Zayed, A.; Terry, N. *Environ. Sci. Technol.* **1998**, *32*, 591.
- Szulcowski, M. D.; Helmke, P. A.; Bleam, W. F. *Environ. Sci. Technol.* **1997**, *31*, 2954–2959.
- Khasim, D. I.; Kumar, N.; Hussain, R. C. *Bull. Environ. Contam. Toxicol.* **1989**, *43*, 742.
- Kortenkamp, A.; Casadevall, M.; Faux, S. P.; Jenner, A.; Shayer, R. O. J.; Woodbridge, N.; O'Brien, P. *Arch. Biochem. Biophys.* **1996**, *329*, 199.
- Katz, S. A.; Salem, H. *The Biological and Environmental Chemistry of Chromium*; VCH Publishers: New York, 1994.
- Wittbrodt, P. R.; Palmer, C. D. *Environ. Sci. Technol.* **1996**, *30*, 2470.
- Hunter, D. Savanna River Ecology Laboratory, personal communication, 1997.
- Mikalsen, A.; Alexander, J.; Wallin, J.; Ingelman-Sundberg, M.; Andersen, R. A. *Carcinogenesis* **1991**, *12*, 825.
- Cupo, D. Y.; Wetterhahn, K. E. *Proc. Natl. Acad. Sci. U.S.A.* **1985**, *82*, 6755.
- deFlora, S. A.; Morelli, A.; Basso, C.; Romano, M. D.; Serra, A. *Cancer Res.* **1985**, *45*, 3188.
- Shi, X.; Dalal, N. S. *Biochem. Biophys. Res. Commun.* **1989**, *163*, 627.
- Banks, R. B.; Cooke, R. T. *Biochem. Biophys. Res. Commun.* **1986**, *137*, 8.
- Standeven, A. M.; Wetterhahn, K. E. *Chem. Res. Toxicol.* **1991**, *4*, 616.
- Connett, P. H.; Wetterhahn, K. E. *Struct. Bonding* **1983**, *54*, 93.
- Shi, X.; Mao, Y.; Knapton, A. D.; King, M.; Roganasakul, Y.; Gannett, P. M.; Dalal, N.; Liu, K. *Carcinogenesis* **1994**, *15*, 2475.
- Stearns, D. M.; Kennedy, L. J.; Courtney, K. D.; Giangrande, P. H.; Phieffer, L. S.; Wetterhahn, K. E. *Biochemistry* **1995**, *34*, 910.
- Shen, H.; Wang, Y.-T. *Appl. Environ. Microbiol.* **1993**, *59*, 3771.
- Turick, C. E.; Apel, W. A.; Carmiol, N. S. *Appl. Environ. Biotechnol.* **1996**, *44*, 683.
- Nies, D. H. *Plasmid* **1992**, *27*, 17.
- Wang, P. C.; Mori, T.; Komori, K.; Sasatsu, M.; Toda, K.; Ohtake, H. *Appl. Environ. Microbiol.* **1989**, *55*, 1665.
- Römhald, V.; Marshner, H. *Plant Physiol.* **1983**, *71*, 949.
- Lyon, G. L.; Peterson, P. J.; Brooks, R. R. *Planta* **1969**, *88*, 282.
- Micera, G.; Dessì, A. *J. Inorg. Biochem.* **1988**, *34*, 157.
- Liu, K. J.; Jiang, J.; Shi, X.; Gabrys, H.; Walczak, T.; Swartz, H. M. *Biochem. Biophys. Res. Commun.* **1995**, *206*, 829.
- Dushenkov, V.; Kumar, P. B. A. N.; Motto, H.; Raskin, I. *Environ. Sci. Technol.* **1995**, *29*, 1239.
- Cotton, A. F.; Wilkinson, G. *Advanced Inorganic Chemistry*, 3rd ed.; Interscience Publishers: New York, 1972; p 830.
- Losi, M. E.; Frankenberger, W. T., Jr. *Water Air Soil Pollut.* **1993**, *74*, 405.
- Chemical Analysis of Water and Waste*; EPA-600/4-79-020; U.S. EPA: Washington, DC, Revised March 1983.
- Kutzler, F. W.; Natoli, C. R.; Misemer, D. K.; Doniach, S.; Hodgson, K. O. *J. Chem. Phys.* **1980**, *73*, 3274.
- Koningsberger, D. C.; Prins, R. *X-ray absorption. Principles, applications and techniques of EXAFS, SEXAFS and XANES*; John Wiley & Sons: New York, 1988.
- Chaney, R. L.; Brown, J. C.; Tiffin, L. O. *Plant Physiol.* **1972**, *50*, 208.
- Zayed, A.; Lytle, C. M.; Qian, J.-H.; Terry, N. *Planta* **1998**, *206*, 293.
- Lytle, F. W. In *Applications of Synchrotron Radiation*; Winick, H., Xian, D., Ye, M., Hyang, P., Eds.; Gordon and Breach: Luxembourg, 1989.
- Rehr, J. J.; Mustre deLeon, J.; Zabinsky, S. I.; Albers, R. C. *J. Am. Chem. Soc.* **1991**, *113*, 5135.
- Zabinsky, S. I.; Rehr, J. J.; Ankudinov, A.; Albers, R. C.; Eller, M. J. *Phys. Rev. B.* **1995**, *52*, 2995.
- Palmer, W. G. *Experimental Inorganic Chemistry*; University Press: Cambridge, 1954.
- Heslop, R. B.; Robinson, P. L. *Inorganic Chemistry*; Elsevier: New York, 1960.
- Polette, L. A.; Gardea-Torresday, J.; Pingitore, N.; Chianelli, R.; Pickering, I.; George, G.; Yacaman, M. J.; AlaTorre, J. A. Presented at SSRL 24th Users' Conference Workshop, Stanford, CA, October, 1997; Paper 6.
- Hermosillo, O. M.; Sarquis, S. *Environ. Technol.* **1990**, *11*, 669.
- Kadlec, R. H.; Knight, R. L. *Treatment Wetlands*; CRC Press: New York, 1996; p 501.
- Reddy, K. R.; Sutton, D. L. *J. Environ. Qual.* **1984**, *13*, 1.

Received for review January 29, 1998. Revised manuscript received June 22, 1998. Accepted June 29, 1998.

ES980089X